Wild-Type and Met-65 → Leu Variants of Human Cystatin A Are Functionally and Structurally Identical[†]

C. Jeremy Craven,[‡] Nicola J. Baxter,[‡] Ewan H. Murray,[‡] Nicola J. Hill,[‡] John R. Martin,[‡] Karin Ylinenjärvi,[§] Ingemar Björk,[§] Jonathan P. Waltho,*[,‡] and Iain A. Murray*[,‡]

Krebs Institute for Biomolecular Research, Department of Molecular Biology and Biotechnology, University of Sheffield, Firth Court, Western Bank, Sheffield S10 2TN, United Kingdom, and Department of Veterinary Medical Chemistry, Swedish University of Agricultural Sciences, Uppsala Biomedical Center, Box 575, SE−751 23 Uppsala, Sweden

Received July 24, 2000; Revised Manuscript Received October 24, 2000

ABSTRACT: The solution structure of an N-terminally truncated and mutant form ($M65L^{2-98}$) of the human cysteine protease inhibitor cystatin A has been reported that reveals extensive structural differences when compared to the previously published structure of full-length wild-type (WT) cystatin A. On the basis of the $M65L^{2-98}$ structure, a model of the inhibitory mechanism of cystatin A was proposed wherein specific interactions between the N- and C-terminal regions of cystatin A are invoked as critical determinants of protease binding. To test this model and to account for the reported differences between the two structures, we undertook additional structural and mechanistic analyses of WT and mutant forms of human cystatin A. These show that modification at the C-terminus of cystatin A by the addition of nine amino acids has no effect upon the affinity of papain inhibition ($K_D = 0.18 \pm 0.02$ pM) and the consequences of such modification are not propagated to other parts of the structure. These findings indicate that perturbation of the C-terminus can be achieved without any measurable effect on the N-terminus or the proteinase binding loops. In addition, introduction of the methionine-65 → leucine substitution into cystatin A that retains the N-terminal methionine ($M65L^{1-98}$) has no significant effect upon papain binding ($K_D = 0.34 \pm 0.02$ pM). Analyses of the structures of WT and $M65L^{1-98}$ using ^{1}H NMR chemical shifts and residual dipolar couplings in a partially aligning medium do not reveal any evidence of significant differences between the two inhibitors. Many of the differences between the published structures correspond to major violations by $M65L^{2-98}$ of the WT constraints list, notably in relation to the position of the N-terminal region of the inhibitor, one of three structural motifs indicated by crystallographic studies to be involved in protease binding by cystatins. In the WT structure, and consistent with the crystallographic data, this region is positioned adjacent to another inhibitory motif (the first binding loop), whereas in $M65L^{2-98}$ there is no proximity of these two motifs. As the NMR data for both WT9C and $M65L^{1-98}$ are wholly consistent with the published structure of WT cystatin A and incompatible with that of $M65L^{2-98}$, we conclude that the former represents the most reliable structural model of this protease inhibitor.

Human cystatin A, also named stefin A, is a member of the cystatin superfamily of cysteine proteinase inhibitors, whose main function is to protect cells from unwanted proteolysis, and is involved in the control mechanism responsible for protein breakdown (*1*). Members of the superfamily are potent competitive inhibitors of papain-like cysteine proteases and have been classified into three subfamilies, based on sequence identity, number of disulfide bonds, and the molecular mass of the proteins (*2*). Cystatin A is classified as a type I inhibitor, contains 98 amino acid residues, has a molecular mass of approximately 11 kDa, and contains no disulfides or carbohydrates. It is believed to provide an important protective function against infective agents (*2*) and has proposed roles in many pathological states including cardiovascular disease and cancer (*3*−*7*). Mutations in the gene encoding cystatin B, a related type I inhibitor (53% amino acid identity with cystatin A), cause a heritable form of progressive myoclonus epilepsy (*8*). While most such mutations are associated with reduced transcription or aberrant splicing of cystatin B RNA (*9*), a single G → C transversion, resulting in the replacement of Gly-4 by arginine, is also sufficient to cause disease (*10*). As this glycine residue is an important determinant of protease inhibition by cystatin A (*11*), and absolutely conserved in all cystatins, it appears that unregulated activity of a papain-like cysteine protease is responsible for this neurodegenerative disorder.

The structure of cystatin B bound to papain has been determined by X-ray crystallography and reveals that three distinct sequence motifs of type I cystatins contribute to protease binding and inhibition (*12*). In the complex, a so-called "tripartite wedge" is formed from the amino terminus (residues Met-1 to Pro-6) and two surface loops (Gln-46 to Asn-52; Leu-73 to Asn-77) of cystatin B. The first loop

[†] We thank the Lister Institute for Preventive Medicine, the Wellcome Trust, the Biotechnology and Biological Sciences Research Council, the British Heart Foundation, and the Swedish Medical Research Council for financial support.

* To whom correspondence should be addressed.
[‡] University of Sheffield.
[§] Swedish University of Agricultural Sciences.

10.1021/bi0017069 CCC: $19.00
Published on Web 12/01/2000

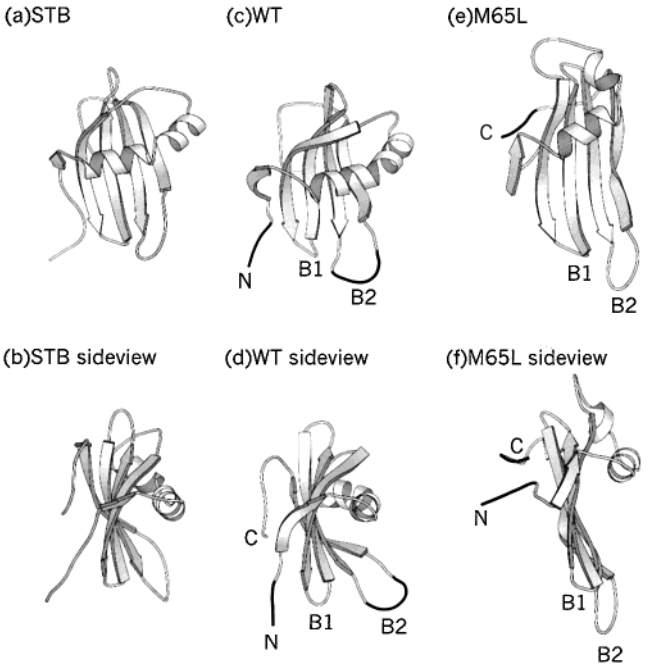

FIGURE 1: Ribbon representations of the structures of cystatin B (STB) (a), wild-type cystatin A (WT) (c) and M65L$^{2-98}$ (M65L) (e) viewed approximately "face-on" to the β-sheet. Panels b, d and f show views approximately orthogonal to those in panels a, c, and e, respectively. Regions that are significantly disordered in cystatin A variants (rmsd to mean > 1.5 Å) are colored black. This figure was created using MOLSCRIPT (33). The N and/or C termini of cystatin A are marked, as are the two loops, B1 and B2, which are identified as being involved in protease binding.

contains the amino acid sequence $Q_{46}VVAG_{50}$ corresponding to the QXVXG motif that is highly conserved throughout the cystatin superfamily. This wedge is highly complementary to the active site cleft of papain and, in the complex, the side chain of the reactive site thiol (Cys-25) of papain is completely encapsulated by residues Ser-3 to Gly-4 of the N-terminal segment and Gln-46 to Val-47 of the first loop. As noted above, cystatin A is highly homologous to cystatin B, and the global fold revealed by the solution structure of wild-type (WT)[1] cystatin A (*13*) is very similar to that of cystatin B bound to papain (rmsd of 1.2 Å for backbone heavy atoms of ordered regions)(Figure 1, panels a−d).

Following the report of the wild-type protein structure (WT:13), a second structure was reported for human cystatin A (*14*), again determined using NMR spectroscopy. The latter was that of a cystatin A variant that lacks the N-terminal methionine group and in which methionine-65 is replaced by leucine (M65L$^{2-98}$). The M65L substitution, created by site-directed mutagenesis of the cystatin A gene, was introduced to facilitate production of cystatin A by cyanogen bromide cleavage of an adenylate kinase-cystatin A fusion protein (*15*). The structures share a common secondary structure organization that consists of a five-stranded antiparallel β-sheet and an α-helical portion. There are, however, a number of significant differences between the reported tertiary structures (Figure 1, panels c−f): (i) In the WT structure, the C-terminal segment lies in a well-defined conformation and is bound against the convex face of the β-sheet. The N-terminal segment forms a looser bundle while making some contact with residues in the first binding loop. In the M65L$^{2-98}$ structure, the positions of both the N- and C-termini differ from those of the WT, and both segments are poorly defined. The N-terminal segment makes no contacts with the first binding loop in the M65L$^{2-98}$ structure. (ii) The single α-helix of the WT inhibitor is effectively continuous with a slight kink. In the M65L$^{2-98}$ structure, this region forms two distinct α-helical segments positioned approximately orthogonal to each other. (iii) In the WT structure, the second binding loop forms a loose bundle. In M65L$^{2-98}$, this loop is tightly defined. (iv) The β-sheet of WT cystatin A is strongly curved around the α-helix. In M65L$^{2-98}$, this β-sheet is flat and the relative disposition of β-sheet and α-helical elements is altered.

NOEs from the C-terminal residues Gly-97 and Phe-98 to Leu-6 are observed for both proteins, prompting the proposal (*14*) that the C-terminus functions to maintain the active conformation of cystatin A via interactions with the N-terminal region. However, such contacts do not extend further into the N-terminal region (residues Met-1 to Gly-5) in either of the cystatin A structures or in cystatin B when bound to papain (*12*). Kinetic studies of papain inhibition by truncated and residue-substituted variants of cystatin A, and other members of the cystatin superfamily, confirm the important contribution of the N-terminal region to protease binding (*11*, *16*−*20*). In contrast, the consequences of C-terminal modification are largely unknown, except that mutation of Tyr-97 in cystatin B results in a 50-fold reduction in its affinity for papain, most likely due to the removal of the direct contact between this residue and the proteinase in the complex (*21*).

In this paper, we consider the M65L$^{2-98}$ structure in the context of the NMR constraints used to determine the structure of WT cystatin A and investigate the possibility that the differences between the two structures arise as a consequence of structure determination at differing pH (pH 5.5 and pH 3.8 for WT and M65L$^{2-98}$, respectively). We address the proposed contribution of interactions between the N- and C-termini to the inhibitory activity of human cystatin A through kinetic and NMR analyses of an inhibitor variant carrying nine additional amino acids at the C-terminus. In addition, using a full-length cystatin A variant containing the Met-65 → Leu substitution, we demonstrate that the extensive differences revealed in a comparison of the published solution structures of WT and M65L$^{2-98}$ variants of cystatin A do not arise as a consequence of the residue substitutions present in the latter.

MATERIALS AND METHODS

Expression of Recombinant Cystatin A. An *Nde*I restriction endonuclease cleavage site was introduced to the 5′-end of the cystatin A coding sequence present in a plasmid previously constructed for the periplasmic expression of cystatin A (*22*). This was achieved by polymerase chain

[1] Abbreviations: WT, wild-type cystatin A; WT9C wild-type cystatin A with nine residue C-terminal extension; M65L$^{1-98}$, cystatin A with Met-65 → Leu substitution; WT$^{2-98}$, cystatin A lacking N-terminal Met-1; M65L$^{2-98}$, cystatin A with Met-65 → Leu substitution and lacking N-terminal Met-1; NMR, nuclear magnetic resonance; NOESY, nuclear Overhauser effect spectroscopy; NOE, nuclear Overhauser effect; HMQC, heteronuclear multiple quantum coherence; TOCSY, total correlation spectroscopy; RDC, residual dipolar coupling; rmsd, root-mean-squared deviation; E-64, *trans*-epoxysuccinyl-L-leucylamido(4-guanidino)-butane.

reaction (PCR) amplification (15 cycles) using oligonucleotides 5′-ACTGTTGCTCAGCATATGATACCTGG-3′ (nucleotides that differ from the original sequence are underlined) and 5′-GCCTGCAGGTCGACTCTAGAG-3′. The latter is complementary to sequences immediately 3′ of a *Bam*HI restriction site located beyond the termination codon of the original plasmid. Amplification products were cleaved with *Nde*I and *Bam*HI and inserted into equivalently cut plasmid pET3a (Novagen) using T4 DNA ligase. Recombinant plasmids were isolated following transformation into *Escherichia coli* JM101 and characterized by DNA sequence analysis throughout the entire cystatin A coding sequence and adjacent vector sequences. This plasmid, pET3a:StefinA, expresses cystatin A in high yield when grown to stationary phase (2YT media, 37 °C) in *E. coli* BL21(DE3) in the absence of induction.

Introduction of a 27-bp 3′-Extension to the Cystatin A Coding Sequence. The cystatin A segment of pET3a:StefinA was reamplified (15 cycles) using the oligonucleotides PET625 (5′-GACTCACTATAGGGAGACC-3′; complement of nucleotides 607−625 of pET3a) and 5′-GGAAGGATCCTAGTGATGATGGTGGTGATGTCCACCGCCAAAGCCCGTCAGCTCGTCATCC-3′, the latter designed to append nine additional codons encoding the sequence $(Gly)_3$-$(His)_6$ (followed by a termination codon and *Bam*HI restriction site) to the 3′-end of the cystatin-coding DNA. PCR products were restricted with *Xba*I (located immediately 5′ of the pET3a T7 RNA polymerase promoter) and *Bam*HI and ligated to equivalently cut pET3a, yielding plasmid pET3a:StefinA:WT9C. Nucleotide sequence analysis was used to confirm introduction of the new sequence and the absence of any additional mutations arising from the PCR.

Site-Directed Mutagenesis. The codon for Met-65 (ATG) of cystatin A was replaced by CTG (Leu) in two stages as follows: First, separate PCR reactions (10 cycles) were carried out using pET3a:StefinA template DNA and oligonucleotides PET625 plus 5′-ACTTTCAA-GTGCAGATATTTATTATC-3′ or PET441 (5′-GGTTATGCTAGTTATTGC-TC-3′; nucleotides 441−460 of pET3a) plus 5′-GATAATAAATATCTGCACTTGAAAGT-3′ and the respective amplification products purified using a GeneClean kit (Bio 101) following agarose gel electrophoresis. Second, these purified products were mixed, reamplified (10 cycles) using oligonucleotides PET440 and PET625, restricted with *Xba*I and *Bam*HI, and ligated to *Xba*I−*Bam*HI-digested pET3a yielding plasmid pET3a:StefinA:$M65L^{1-98}$. As previously, the nucleotide sequence of the inserted DNA fragment was determined prior to recombinant expression and protein characterization.

Purification of Recombinant Cystatin A. Stationary-phase *E. coli* BL21(DE3) cells containing cystatin A expression vectors were harvested by centrifugation, resuspended in cold potassium phosphate buffer (50 mM, pH 6.5) containing protease inhibitors (0.1 mM phenanthroline, 0.1 mM dichloroisocoumarin, 20 μM E-64), lysed by ultrasonic disruption and cell-free extracts were prepared by centrifugation (15 000 rpm, 45 min, 4 °C). Wild-type and $M65L^{1-98}$ cystatin A variants were purified by affinity chromatography on S-(carboxymethyl)papain-agarose (*22*) followed by anion-exchange chromatography using Q-Sepharose (Pharmacia). Cystatin A WT9C was purified by immobilized-metal affinity chromatography using Ni^{2+}-NTA resin (Qiagen). The concentration of purified cystatin A preparations was determined by measuring UV absorbance at 280 nm (extinction coefficient = 8800 M^{-1} cm^{-1}; 21). For the preparation of cystatin A uniformly enriched with ^{15}N, LB broth was replaced by M9 media containing 1 g/L of $(^{15}NH_4)_2SO_4$ as the sole nitrogen source, as previously described (*23*).

Spectroscopic Methods. Cystatin A samples were concentrated to ∼2mM, and the pH was adjusted by addition of small amounts of HCl or NaOH, buffered with acetate (for pH values < 5.5) or phosphate (pH values > 5.5). NMR spectra were acquired at 308 K on Bruker AMX500 or DRX500 spectrometers. The HMQC spectra were acquired with a jump-return sequence for solvent suppression, acquiring 128 complex pairs in the indirect dimension, with spectral widths of 12 500 Hz in the proton dimension and 1667 Hz in the nitrogen dimension. NOESY and TOCSY spectra were acquired as described in Martin et al. (*13*) with mixing times of 150 and 90 ms, respectively. Proton chemical shifts were calculated using the program TOTAL (*24*), which directly calculates the proton shifts based on atomic coordinates using an empirical formula. Complete resonance assignment of WT9C and $M65L^{1-98}$ was carried out using methods described previously for WT cystatin A (*13*). Residual dipolar couplings (*25*) were measured at 308 K using solutions of ^{15}N-labeled WT (0.4 mM) and $M65L^{1-98}$ (0.5 mM) cystatin A in 50 mM potassium phosphate buffer/0.2M NaCl (pH 5.5) containing 2.4% (w/v) cetylpyridinium chloride/hexanol (1:1 w/w) as the alignment medium (*26*). Residual dipolar couplings ranging in value from +15.9 Hz to −7.4 Hz were observed using J-coupled ^1H,^{15}N-HSQC spectra (*27*).

Inhibition Studies. Papain (EC 3.4.22.2) was prepared and stored as previously described (*28*). Association rate constants, k_{ass}, for the interactions of cystatin A variants with papain were evaluated under pseudo-first-order conditions at different inhibitor concentrations by continuous measurements of the loss of enzyme activity against a fluorogenic substrate (*19*). Dissociation rate constant, k_{diss}, of complexes between cystatin A variants and papain were measured by trapping the enzyme dissociating from the complex by an excess of chicken cystatin, which forms a much tighter complex with papain than does cystatin A (*19, 22*). The dissociation rate was monitored by the appearance of the tight chicken cystatin−papain complex, analyzed by ion-exchange HPLC (*29*). Dissociation equilibrium constants, K_D, were calculated as k_{diss}/k_{ass}.

RESULTS

Comparison of Cystatin A Structures. The differences revealed in the two published structures of cystatin A prompted us to reexamine the NMR constraints used to calculate the WT structure (*13, 23*) to assess whether they were compatible with the $M65L^{2-98}$ structure (*14*). Were this the case, it would indicate that our structure calculation was based on insufficient sampling of conformational space and that we had only identified a subset of the full family of structures that are consistent with our data. In fact, we find that very many WT constraints are *not* consistent with $M65L^{2-98}$ and Figure 2, panel c, shows those WT constraints, superimposed on the structure of $M65L^{2-98}$, that correspond to distances in excess of 12 Å in the latter. In Figure 2, we also show examples of NOESY peaks that correspond to some of these constraints (Figure 2, panels d−f) and the

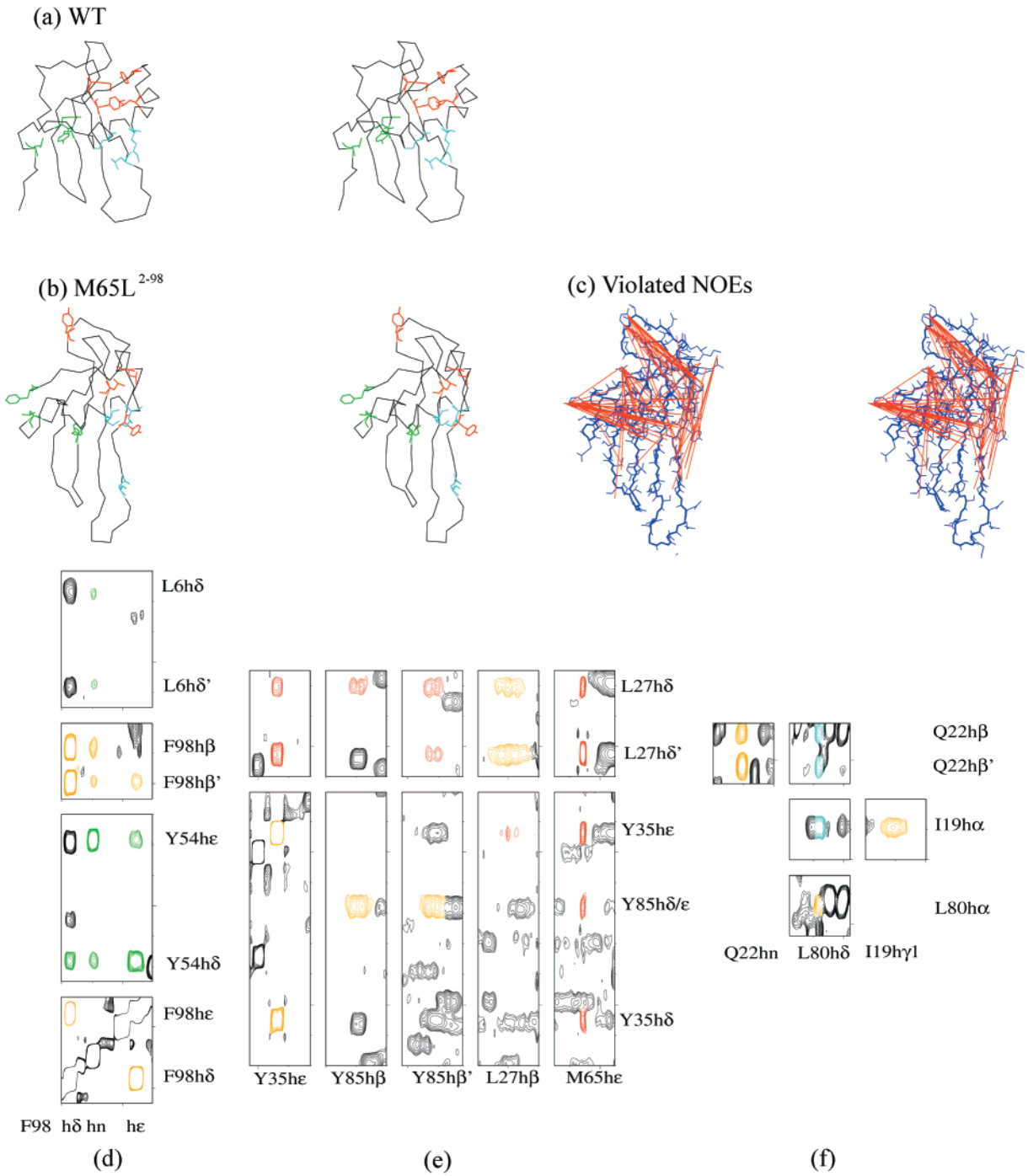

FIGURE 2: Interactions between key residues in the WT structure. In panels d−f, inter- and intraresidue cross-peaks are shown, corresponding to interactions between the groups shown in stereoviews of the WT (a) and M65L$^{2-98}$ (b) structures. Interresidue cross-peaks are colored according to the color scheme used in panels a and b, while intraresidue cross-peaks (which are shown to corroborate the interresidue cross-peak assignments) are colored gold. Stereoviews panels a and b show the backbone for all residues in black, and the side chain residues of certain key amino acids are colored according to structural significance. Within each color group, intermolecular NOEs are observed in the WT spectra. Residues L6, F98, and Y54, which are significant in restraining the N- and C-termini are colored green. Residues L27, Y35, M65, and Y85, which are located in or near the loop region linking the α-helix to the β-sheet, are colored red. Residues I19, K22, and L80, which are involved in constraints that wrap the β-sheet around the α-helix, are colored blue. (c) Stereoview of the M65L$^{2-98}$ structure showing, in red, the distribution and extent of constraints from the WT constraints list that are inconsistent with the M65L$^{2-98}$ structure. All heavy atoms are shown, with the backbone highlighted by a thicker line. The constraints shown are those that correspond to a distance greater than 12 Å in the M65L$^{2-98}$ structure. These constraints play a major role in defining the β-sheet twist and the overall compactness of the WT structure.

positions of the relevant amino acids within the WT (Figure 2, panel a) and M65L$^{2-98}$ (Figure 2, panel b) structures.

pH Titration. To assess whether the structural differences between WT and M65L$^{2-98}$ arise as a consequence of structure determination at differing pH we collected a series of 1D ^{1}H and 2D ^{15}N-^{1}H correlation (HMQC) spectra at pH values 7.5, 7, 6.5, 6, 5.5, 4.5, and 3.6. 2D ^{1}H NOESY and TOCSY data were acquired at pH 3.7 and also reacquired at pH 5.5 using the same sample under otherwise identical conditions. The chemical shift changes observed in the

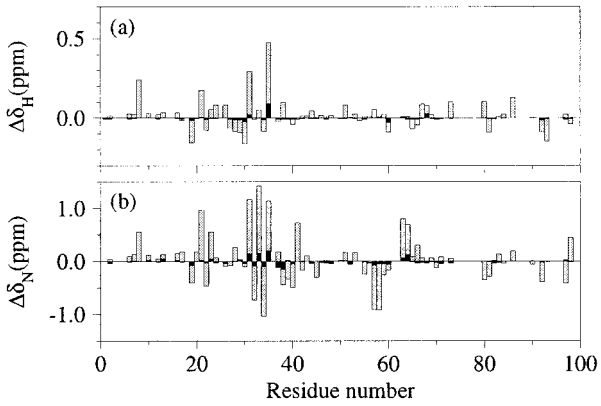

FIGURE 3: Chemical shift changes for WT cystatin A on varying the pH: (a) amide protons resonances and (b) amide nitrogen resonances. For each resonance, the chemical shift change on varying the pH from 7.5 to 5.5 is shown as a black bar, and the change on varying the pH from 5.5 to 3.6 is shown as a gray bar. The resonance for Y35 could not be relocated at pH 3.6, and the change shown is for pH 4.5. Other resonances that could not be unambiguously followed, or which were strongly attenuated at the upper pH, are omitted from the diagram.

HMQC spectra from the titration series are summarized in Figure 3. The pH range is divided into two: pH 7.5 to 5.5, i.e., above and down to the pH of the WT structure determination, and pH 5.5 to 3.6, i.e., from the pH of the WT structure determination down to the pH used to study M65L$^{2-98}$. The total changes in chemical shift across the full pH range studied are very similar to those reported for a similar titration using M65L$^{2-98}$ (*14*), predominantly occurring around residue Tyr-35 in the loop region joining the α-helix and the β-sheet. Such changes that do occur do so predominantly in the pH range 5.5 to 3.6, while the spectra at the higher pHs overlay very closely. The overlay of spectra shown in Figure S-5 of the Supporting Information of Tate et al. (*14*) show that this is also the case for M65L$^{2-98}$, confirming that the structure in the loop region around Tyr-35 is sensitive to pH between pH 5.5 and 3.8. In contrast, we observe no change in the chemical shift of the strongly upfield-shifted methyl resonances of Ile-16 and Ile-19 between pH 5.5 and 3.7, indicating that the tertiary interactions that give rise to these shifts are maintained.

Effect of C-Terminal Modification of Cystatin A. The cystatin A variant WT9C, which contains nine additional amino acid residues [(Gly)$_3$-(His)$_6$] appended to the C-terminal residue (Phe-98) of the WT inhibitor, was constructed to investigate the functional and structural consequences of modification of the carboxyl-terminus. PCR amplification was used to introduce nine additional in-frame codons to the 3′-end of the gene encoding WT. WT9C protein was purified to homogeneity, as assessed by SDS−PAGE analysis, by immobilized metal affinity chromatography. Association and dissociation rate constants for the interaction of WT9C and papain are presented in Table 1. The K_D value calculated from the measured rate constants is identical (0.18 ± 0.02 pM) to that determined previously for papain binding by the WT inhibitor (*21*), indicating that the C-terminal extension does not compromise the inhibitory capacity of cystatin A. Similarly, the C-terminal extension does not perturb the structure away from that reported for the WT inhibitor. This is illustrated, for example, in Figure 4, panel a, which shows the distribution of ^{1}H chemical shift differences of backbone resonances between WT and WT9C variants. With the exception of resonances associated with the additional residues of WT9C, significant changes are limited to minor perturbations of residues 97 and 98, the point of attachment of the (Gly)$_3$-(His)$_6$ extension. Notably, no significant changes are observed for nuclei close to where the side chain of Phe-98 packs against the β-sheet, those close to where the α-helix packs against the opposite side of the β-sheet, or those of the N-terminal residues. The line widths of the ^{1}H resonances corresponding to the (Gly)$_3$-(His)$_6$ extension indicate that all of these residues have a mobility that is independent of the remainder of the protein.

Table 1: Association and Dissociation Rate Constants and Dissociation Equilibrium Constants Determined for the Interaction of WT, WT9C, and M65L$^{1-98}$ Variants of Cystatin A with Papain[a]

cystatin A variant	k_{ass} (M^{-1} s^{-1})	k_{diss} (s^{-1})	K_D (pM)
WT[b]	$3.1 \pm 0.05 \times 10^6$	$5.5 \pm 0.5 \times 10^{-7}$	0.18 ± 0.02
WT9C	$2.4 \pm 0.03 \times 10^6$	$4.4 \pm 0.3 \times 10^{-7}$	0.18 ± 0.02
M65L$^{1-98}$	$2.1 \pm 0.10 \times 10^6$	$7.4 \pm 0.4 \times 10^{-7}$	0.34 ± 0.04

[a] Kinetic parameters were determined as described in Materials and Methods. [b] WT data are from previous work (*21*).

Effect of Met-65 → Leu Substitution. PCR-based site-directed mutagenesis was used to introduce a leucine codon at position 65 in place of the methionine codon normally present in the gene encoding WT cystatin A. The encoded cystatin A variant M65L$^{1-98}$ was purified to homogeneity by a combination of carboxymethylpapain-agarose affinity and anion exchange chromatography. Association and dissociation rate constants for the interaction of M65L$^{1-98}$ and papain are presented in Table 1. In this case, a slight increase (less than 2-fold) in calculated K_D was observed (0.34 ± 0.04 pM) when compared with WT cystatin A, the change arising as a result of small changes in both association and dissociation rate constants. This minor decrease in affinity is consistent with only very minimal perturbations of the binding region. In agreement, there is no significant change in the structure of the M65L$^{1-98}$ variant as compared with that reported for WT. In Figure 4, panel b, is shown the distribution of ^{1}H chemical shift differences of backbone resonances between WT and M65L$^{1-98}$ variants. In this instance, chemical shift differences were limited to very small changes in nuclei located in close proximity to the site of the Met → Leu substitution and were not propagated significantly to other parts of the structure. As reported for the WT9C variant, no significant changes are observed for nuclei of the N-terminal residues. While it is possible that the conformational perturbation reported in the M65L$^{2-98}$ study by coincidence leads to only very small chemical shift differences of the type observed here, this would not be expected from the changes in chemical shift calculated for the WT and M65L$^{2-98}$ structures using the program TOTAL (*24*). However, to assess this possibility experimentally, we measured the residual dipolar couplings (RDC) between backbone amide hydrogen and nitrogen nuclei for both WT and M65L$^{1-98}$ variants while partially aligned in solutions containing cetylpyridinium chloride-hexanol lamellae. In Figure 5 the observed RDC values for the two proteins are plotted against each other. The closeness of the correlation indicates that the backbone conformations of the two proteins are virtually identical.

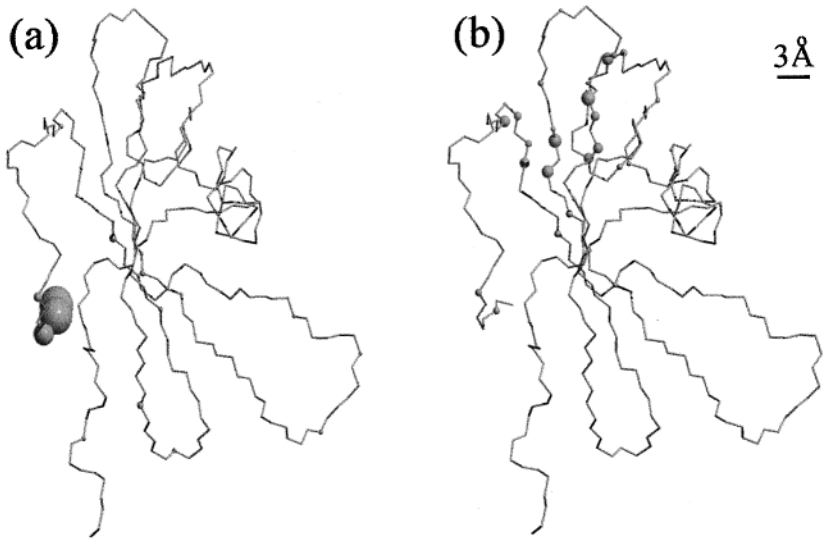

FIGURE 4: ^{1}H chemical shift changes relative to WT cystatin A observed for the backbone resonances of (a) variant WT9C and (b) variant M65L$^{1-98}$. The size of the spheres shown are proportional to the observed chemical shift changes (a diameter of 1 Å is equivalent to a chemical shift change of 0.12 ppm). A scale bar corresponding to a length of 3 Å (δ = 0.36 ppm) is shown for comparison.

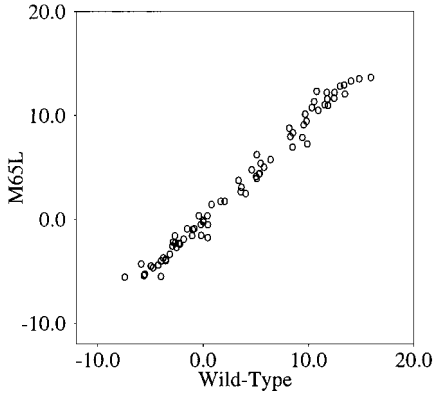

FIGURE 5: A correlation plot of the ^{1}H-^{15}N residual dipolar coupling values (in Hz) measured for WT and variant M65L$^{1-98}$ cystatin A under identical conditions. Each symbol corresponds to the backbone amide group of individual residues distributed throughout the protein. The very high correlation shows that the structures are essentially identical.

DISCUSSION

A reexamination of the NMR constraints used to calculate the solution structure of WT cystatin A confirms that they are incompatible with the published structure of M65L$^{2-98}$ (Figure 2, panel c) and indicates that the differences between the two structures are not simply a consequence of insufficient sampling of conformational space in the original study (*13*). Similarly, the major differences between the two cystatin A structures cannot be attributed solely to the different pH values at which spectra were collected: pH 5.5 for WT (*13*) and pH 3.8 for M65L$^{2-98}$ (*14*). Although there is evidence of a localized pH-dependent change in the studies of both WT (Figure 3) and M65L$^{2-98}$ (*14*), in each case this is limited to the loop region centered on Tyr-35. We found no evidence, for example, for pH-dependent changes in the upfield-shifted methyl resonances associated with residues Ile-16 and Ile-19 of the WT inhibitor. These signals report on the interactions between aromatic rings of Tyr-43 and Tyr-53 in the β-sheet and methyl groups in the α-helix, indicating that the relative configuration of the two major elements of secondary structure is unperturbed across the pH range 3.7−5.5. The primary change with pH is that the excellent quality of NOESY and TOCSY spectra obtained at pH 5.5, as expected from a protein with such a short correlation time (4.5 ns), is severely degraded at pH 3.7. Recently, cystatin A has also been shown to undergo a well-defined dimerization reaction under conditions in which the native fold is strongly destabilized (*30*), in a manner similar to that reported previously for the type II inhibitor, cystatin C (*31*, *32*). However, the introduction of this structural perturbation is again insufficient to account for the structure reported for M65L$^{2-98}$. In both dimerization reactions, NMR chemical shift perturbations are limited to a few residues in the N-terminus and the two proteinase binding loops (*30*, *32*) and are not propagated throughout the β-sheet, the α-helix, or the C-terminus.

Another possible explanation for the structural differences between WT and M65L$^{2-98}$ is the presence of two sequence alterations in the latter, namely, absence of the N-terminal methionine residue and the replacement of Met-65 by Leu. We have previously shown that the former change has no significant effect on binding to papain (*19*). This finding indicates that the amino-terminal residue of cystatin A neither makes any relevant contribution to the interaction with this protease nor is its deletion responsible for the structural changes reported for M65L$^{2-98}$. The very high mobility of Met-1 and Ile-2 observed in the WT structure (*13*) provides strong support for this argument. Regarding the Met-65 → Leu substitution, in WT cystatin A this residue forms part of the hydrophobic core at the interface between the β-sheet and α-helix (*13*) as does the equivalent residue (Val-65) in cystatin B (*12*). Introducing the same substitution into full-length cystatin A to produce variant M65L$^{1-98}$ has minimal effects on the kinetics and affinity of protease inhibition (K_D increases from 0.18 to 0.34 pM; Table 1), indicating again that any structural changes arising from the amino acid alteration are not manifested in reduced inhibitory capacity. The combination of limited perturbation of ^{1}H NMR chemical shifts and backbone ^{1}H-^{15}N residual dipolar couplings indicates that virtually no changes in overall conformation are introduced by the Met-65 to leucine substitution. The

small changes that do occur, reflected by the small chemical shift changes (Figure 4, panel b), are likely to fall within the resolution of the structure previously determined for the WT protein and are restricted to the immediate vicinity of Leu-65. They are not propagated to α-helix bending, β-sheet flattening, a loss of contacts between helix and sheet, or a distortion of the three motifs that form the protease-binding surface of the inhibitor. We therefore find no evidence that either residue alteration causes a transition toward a structure resembling that reported for M65L$^{2-98}$ (*14*).

From a functional perspective, the most important difference between the two structures relates to the position of the N-terminal region. The degree of structure in these segments is, despite statements to the contrary (*14*), very similar with a backbone rmsd of approximately 1 Å for Gly-5 in both structures, which rises steeply toward the N-terminus. The position of the two N-termini is, however, very different. Residues Gly-4 to Leu-6 are located adjacent to the first binding loop in WT but distant from this loop in M65L$^{2-98}$. Close contacts between residues of the N-terminal "trunk" and of the first binding loop are also present in the structure of cystatin B in complex with papain (*12*).

The importance of the N-terminal residues of cystatin A in cysteine protease binding has been addressed by engineered truncation and site-directed mutagenesis experiments. Replacement of Gly-4, a conserved residue within the cystatin superfamily, by alanine, serine, or tryptophan reduces papain affinity by 3, 4, and 6 orders of magnitude, respectively (*11*), while deletion of one, two, or three N-terminal residues reduces papain affinity by 0, 3, and 6 orders of magnitude (*19*). These findings are largely in contrast to those of earlier studies of similarly modified cystatins that often yielded different or contradictory results, primarily owing to the use of less appropriate equilibrium methods in determining binding constants for such tight binding inhibitors (reviewed in ref *11*). Given the reported affinity of cystatin A for papain (*22*) and these large reductions in the papain binding affinities of N-terminally modified variants of cystatin A, it is surprising that M65L$^{2-98}$ was claimed to be "fully active" against papain (*14*). In fact, the K_i value of 2.45 nM reported for M65L$^{2-98}$ (*18*), though almost identical to that determined for wild-type cystatin A (1.20 nM) by the same unsuitable equilibrium method, is 4 orders of magnitude higher than the value of 0.18 pM measured by a more appropriate method (*22*). However, the results reported here for M65L$^{1-98}$ and previously for variant WT$^{2-98}$ (*19*) suggest that in all probability M65L$^{2-98}$ is as effective an inhibitor as WT, a conclusion that is not readily reconciled with the dramatic change in position of the N-terminal region reported for M65L$^{2-98}$ (*14*).

It was also proposed (*14*) that "the conformation of the first binding loop (the active conformation) is maintained by specific interactions between the N- and C-termini and is transformed into the inactive conformation by removing the N- and C-interterminal interactions". This proposal arises directly from the observation in the M65L$^{2-98}$ structure that the N- and C-terminal segments are located adjacent to each other. Their relationship is markedly different to that present in the WT structure (Figure 1). We chose to address the significance of interactions between these regions by analyzing the structural and functional consequences of targeted modification of the C-terminus. While this could, in principle, be achieved by amino acid truncation we chose instead to add amino acids to the C-terminus. This was because the side chain of the C-terminal residue (Phe-98) of both WT cystatin A (*13*) and cystatin B (*12*) is packed against a hydrophobic patch at the back of the β-sheet, and we reasoned that removing this interaction would likely destabilize the overall fold of the inhibitor irrespective of any possible effect upon interactions involving the N-terminus.

The variant WT9C, containing nine additional amino acids at the C-terminus, was found to inhibit papain with essentially the same kinetics and affinity as WT (Table 1). Consistent with this observation, comparison of ^{1}H NMR spectra of WT and WT9C reveals no significant changes in structure other than minor perturbation of Gly-97 and Phe-98, residues immediately adjacent to the point of C-terminal extension (Figure 4, panel a). Significantly, we find no evidence that these structural changes are propagated to the N-terminal region and, therefore, no evidence for the proposed relationship (*14*) between the N- and C-termini. In this context, it should be noted that, while the C-terminal region of WT is well-defined by NOEs from Leu-95 and Phe-98 to several residues within the β-sheet (see for example Figure 2, panel c), the four C-terminal residues of M65L$^{2-98}$ have very high rmsd values indicating that this region is relatively undefined in this structure.

In conclusion, we have demonstrated that neither variations in pH nor the presence of either of the two sequence changes found in M65L$^{2-98}$ have any significant effect upon the structure and/or inhibitory properties of cystatin A. Also, our structural data for the WT9C and M65L$^{1-98}$ variants are fully consistent with the WT structure and provide no evidence for the existence of an alternative structure of the type reported for M65L$^{2-98}$ within the normal solution behavior of cystatin A.

SUPPORTING INFORMATION AVAILABLE

Diagonal plot for the WT structure showing the constraints used in the calculations and short distances within the resulting structure (Figure S-1). This material is available free of charge via the Internet at http://pubs.acs.org.

REFERENCES

1. Turk, V., and Bode, W. (1991) *FEBS Lett. 285*, 213−219.
2. Barrett, A. J., Rawlings, N. D., Davies, M. E., Machleidt, W., Salvesen, G., and Turk, V. (1986) In *Proteinase Inhibitors* (Barrett, A. J., and Salvesen, G., eds) pp 515−569, Elsevier, Amsterdam.
3. Rinne, A. (1979) *Acta Univ. Oulu. D41, Anat. Pathol. Microbiol. 4*.
4. Rinne, A., Järvinen, M., Räsänen, O., and Dorn, A. (1980) *Acta Histochem.*, Suppl. *22*, 325−329.
5. Lah, T. T., Kokalj-Kunovar, M., and Turk, V. (1990) *Biol. Chem. Hoppe-Seyler 371*, 199−203.
6. Hopsu-Havu, V. K., Järvinen, M., and Rinne, A. (1983) *Br. J. Dermatol. 109*, 77−85.
7. Hopsu-Havu, V. K., Joronen, I., Järvinen, M., and Rinne, A. (1983) *Eur. Rev. Med. Pharm. Sci. 5*, 1−4.
8. Pennacchio, L. A., Lehesjoki, A. E., Stone, N. E., Willour, V. L., Virtaneva, K., Miao, J. M., Damato, E., Ramirez, L., Faham, M., Koskiniemi, M., Warrington, J. A., Norio, R., Dela-Chapelle, A., Cox, D. R., and Myers, R. M. (1996) *Science 271*, 1731−1734.
9. Lehejoski, A. E., and Koskiniemi, M. (1999) *Epilepsia 40*, 23−28.

10. Lalioti, M. D., Mirotsou, M., Buresi, C., Peitsch, M. C., Rossier, C., Ouazzani, R., Baldy-Moulinier, M., Bottani, A., Malafosse, A., and Antonarakis, S. E. (1997) *Am. J. Hum. Genet. 60*, 342−351.
11. Estrada, S., Nycander, M., Hill, N. J., Craven, C. J., Waltho, J. P., and Björk, I. (1998) *Biochemistry 37*, 7551−7560.
12. Stubbs, M. T., Laber, B., Bode, W., Huber, R., Jerala, R., Lenarcic, B., and Turk, V. (1990) *EMBO J. 9*, 1939−1947.
13. Martin, J. R., Craven, C. J., Jerala, R., Kroon-Zitko, L., Zerovnik, E., Turk, V., and Waltho, J. P. (1995) *J. Mol. Biol. 246*, 331−343.
14. Tate, S., Ushioda, T., Utsunomiya-Tate, N., Shibuya, K., Ohyama, Y., Nakano, Y., Kaji, H., Inagaki, F., Samejima, T., and Kainosho, M. (1995) *Biochemistry 34*, 14637−14648.
15. Kaji, H., Samejima, T., Kumagai, I., Hibino, T., Miura, K., and Takeda, A. (1990) *Biol. Chem. Hoppe-Seyler 371*, Suppl., 145−150.
16. Björk, I., Pol, E., Raub-Segall, E., Abrahamson, M., Rowan, A. D., and Mort, J. S. (1994) *Biochem. J. 299*, 219−225.
17. Björk, I., Brieditis, I., and Abrahamson, M. (1995) *Biochem. J. 306*, 513−518.
18. Shibuya, K., Kaji, H., Itch, T., Ohyama, Y., Tsujikami, A., Tate, S., Takeda, A., Kumagai, I., Hirao, I., Miura, K., Inagaki, F., and Samejima, T. (1995) *Biochemistry 34*, 12185−12192.
19. Estrada, S., Pavlova, A., and Björk, I. (1999) *Biochemistry 38*, 7339−7345.
20. Ylinenjärvi, K., Widersten M., and Björk, I. (1999) *Eur. J. Biochem. 261*, 682−688.
21. Pol, E., and Björk, I. (1999) *Biochemistry 38*, 10519−10526.
22. Pol, E., Olsson, S.-L., Estrada, S., Prasthofer, T. W., and Björk, I. (1995) *Biochem. J. 311*, 275−282.
23. Martin, J. R., Jerala, R., Kroon-Zitko, L., Zerovnik, E., Turk, V., and Waltho, J. P. (1994). *Eur. J. Biochem. 225*, 1181−1194.
24. Williamson, M. P., and Asakura, T. (1993) *J. Magn. Reson. B 101*, 63−71.
25. Tjandra, N., and Bax, A. (1997) *Science 278*, 1697.
26. Prosser, R. S., Losonczi, J. A., and Shiyanovskaya, I. V. (1998) *J. Am. Chem. Soc. 120*, 11010−11011.
27. Ottiger, M., Delaglio, F., and Bax, A. (1998) *J. Magn. Reson. 131*, 373−378.
28. Lindahl, P., Alriksson, E., Jörnvall, H., and Björk, I. (1988) *Biochemistry 27*, 5074−5082.
29. Lindahl, P., Abrahamson, M., and Björk, I. (1992) *Biochem. J. 281*, 49−55.
30. Jerala, R, and Zerovnik, E. (1999) *J. Mol. Biol. 291*, 1079−1089.
31. Ekiel, I., and Abrahamson, M. (1996) *J. Biol. Chem. 271*, 1314−1421.
32. Ekiel, I., Abrahamson, M., Fulton, D. B., Lindahl, P., Storer, A. C., Levadoux, W., Lafrance, M., Labelle, S., Pomerleau, Y., Groleau, D., LeSauteur, L., and Gehring, K. (1997) *J. Mol. Biol. 271*, 266−277.
33. Kraulis, P. J. (1991) *J. Appl. Crystallogr. 24*, 946−950.

BI0017069